Electronic Supplementary Information

Light-Responsive Pickering Emulsions Based on Azobenzene-Modified Silica Particles

Kieran D. Richards[a] *and Rachel C. Evans*[a]*

[a] Department of Materials Science & Metallurgy, University of Cambridge, 27 Charles Babbage Road, CB3 0FS, U.K.

* Corresponding Author: rce26@cam.ac.uk

TABLE OF CONTENTS

1 Characterisation of Synthesised Azobenzene Derivatives

1.1. NMR spectroscopy

^{1}H NMR and ^{13}C NMR spectra were obtained using a Bruker 400 MHz QNP Cryoprobe nuclear magnetic resonance (NMR) spectrometer. Samples were prepared by dissolving 40 mg of sample in 0.7 ml of d-chloroform.

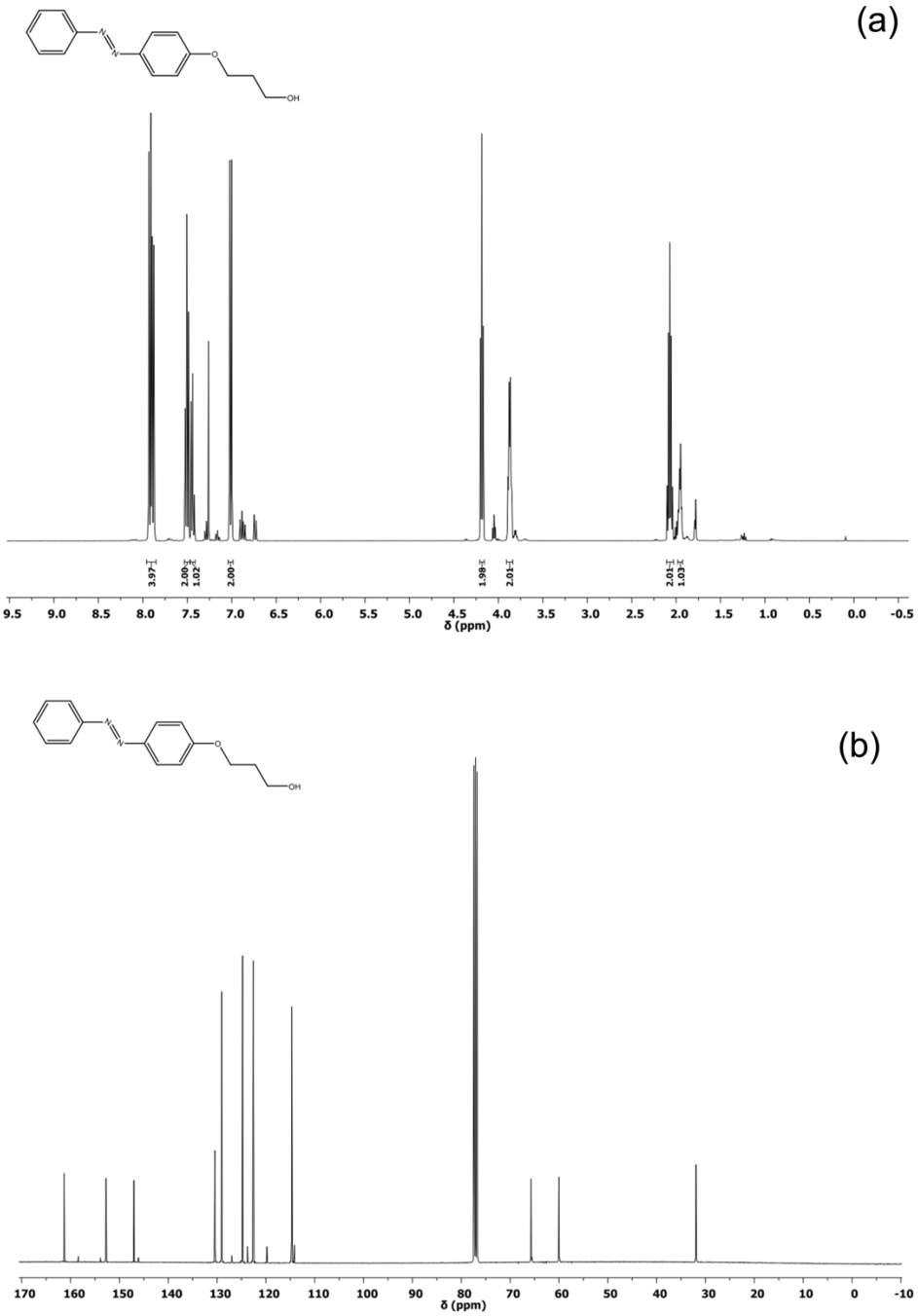

Figure S1. (a) ^{1}H NMR and (b) ^{13}C NMR spectra of $AzoO(CH_2)_3OH$ measured in d-chloroform at 400 MHz and 100 MHz, respectively.

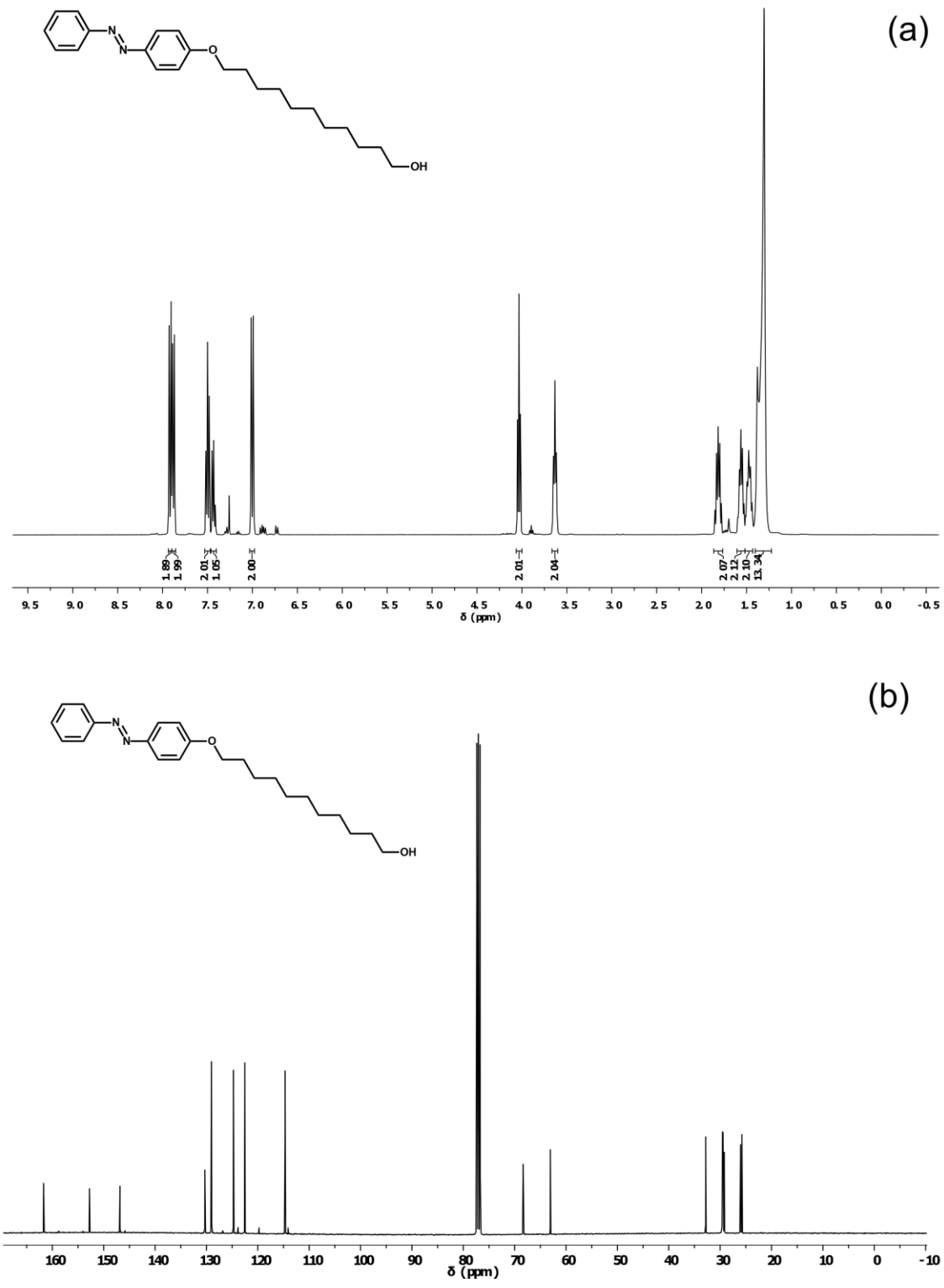

Figure S2. (a) ^{1}H NMR and (b) ^{13}C NMR spectra of Azo$(CH_2)_{11}$OH measured in d-chloroform at 400 MHz and 100 MHz, respectively.

1.2. Mass Spectrometry

Mass spectra were obtained using a Waters LCT Premier Time of Flight mass analyser with W optics. Samples were prepared using 50% aqueous acetonitrile with 0.25% formic acid as a mobile phase and ionised using the electrospray (ESI) technique.

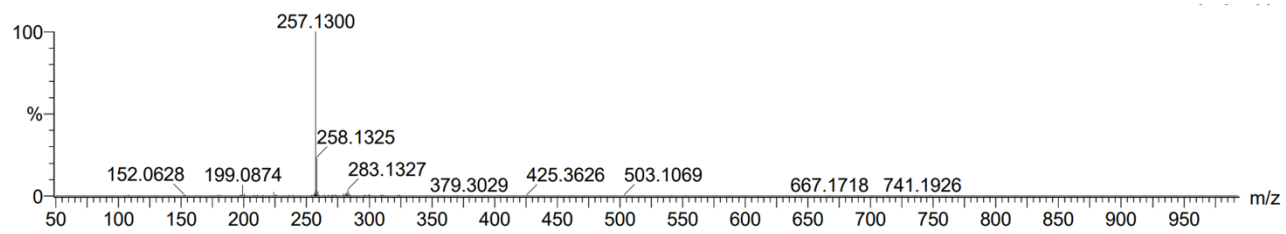

Figure S3. Mass spectrum of Azo$(CH_2)_3OH$. *m/z* $[M+H^+]$ $C_{15}H_{17}N_2O$: calc. 257.1245; found 257.1300.

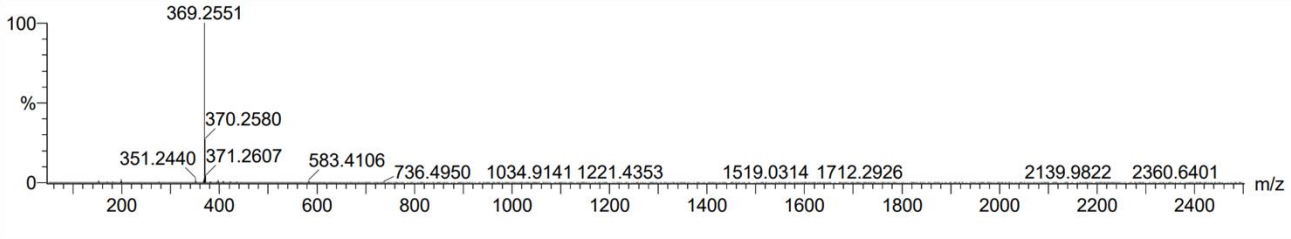

Figure S4. Mass spectrum of Azo$(CH_2)_{11}OH$. *m/z* $[M^+H^+]$ $C_{23}H_{33}N_2O_2$: calc. 369.2497; found 369.2551.

2 Characterisation of Azo-Modified Fumed Silica

2.1 UV/Vis absorption and reflectance spectroscopy

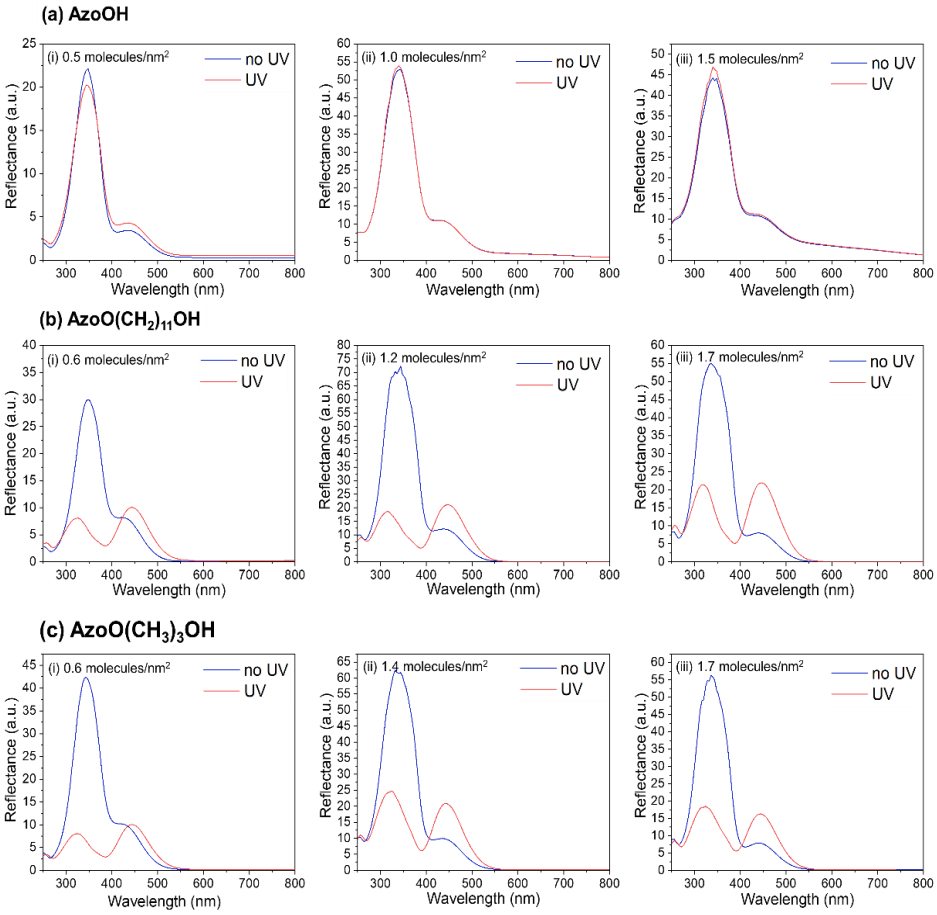

Figure S5. Diffuse reflectance UV/Vis (DRUV) spectra confirming the presence of azobenzene derivatives on the surface of fumed silica and showing isomerisation in response to UV light. Spectra are of (a) AzoOH-silica, (b) AzoO$(CH_2)_3$OH-silica and (c) AzoO$(CH_2)_{11}$OH-silica modified at three different grafting densities (i, ii, and iii) measured before (blue line) and after (red line) UV irradiation (365 nm, 6.00 mW cm^{-2} irradiance, 20 min).

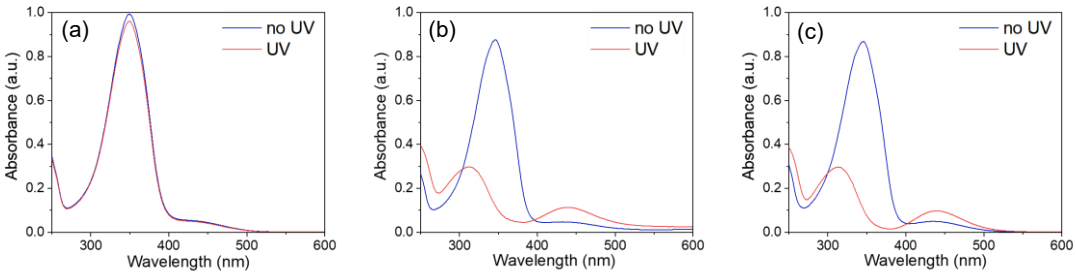

Figure S6. UV/Vis absorption spectra of (a) AzoOH, (b) Azo$(CH_2)_3$OH and (c) Azo$(CH_2)_{11}$OH in isopropyl alcohol (0.04 mmol L^{-1}) after dark storage and before UV irradiation (blue lines) and after 20 min irradiation with UV light (red lines).

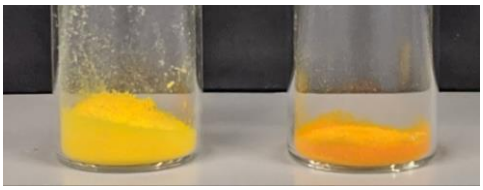

Figure S7. Photograph of AzoO$(CH_2)_{11}$OH-silica-(1.4 molecules/nm^2) showing the colour change observed from yellow (left) before irradiation to orange (right) after irradiation with UV light for 20 min.

Determination of the photostationary state (PSS) composition:

The degree of photoisomerisation in the *cis*-photostationary state (PSS) was calculated from the ratio of the *cis*-PSS absorbance to 100% trans-isomer absorbance (or reflectance), at a given wavelength from:[1]

$$ID_{trans-cis} = \frac{A(0)_{350} - A(PSS)_{350}}{A(0)_{350}} \times 100\% \quad \text{(S1)}$$

where $A(0)_{350}$ refers to the absorbance of 100% *trans*-isomers at 350 nm and $A(PSS)_{350}$ refers to the absorbance of the *cis*-PSS at 350 nm.

Table S1. Photostationary state composition (%*cis*) for Azo derivatives in isopropyl alcohol (0.04 mmol L^{-1}). Absorbance values at 350 nm obtained from UV/Vis absorption spectra measured before and after irradiation with UV light (see Figure S5). Switching to a *cis*-dominant state is seen for Azo$(CH_2)_3$OH and Azo$(CH_2)_{11}$OH.

Azo	**Absorbance (a.u.) (350 nm) No UV**	**Absorbance (a.u.) (350 nm) UV**	**PSS (% *cis*)**
AzoOH	0.99	0.96	3
AzoO$(CH_2)_3$OH	0.86	0.098	88
AzoO$(CH_2)_{11}$OH	0.84	0.075	91

Table S2. Calculation of photostationary state (PSS) composition (%*cis*) for Azo-silica particles from DRUV spectra before and after irradiation with UV light (Figure 56). Switching to a *cis*-dominant state is seen for Azo$(CH_2)_3$OH-silica and Azo$(CH_2)_{11}$OH-silica particles, in agreement with data in Table S1 for the analogous Azo molecules in solution.

Azo	Azo grafting density (molecules/nm^2 (EA))	Reflectance (a.u.) (350 nm) no UV	Reflectance (a.u.) (350 nm) UV	PSS (% *cis*)
AzoOH-silica	0.5	22.11	20.15	9
AzoOH-silica	1.0	51.79	52.15	0
AzoOH-silica	1.5	43.35	45.05	0
AzoO$(CH_2)_3$OH-silica	0.6	29.93	5.87	80
AzoO$(CH_2)_3$OH-silica	1.4	68.83	11.06	84
AzoO$(CH_2)_3$OH-silica	1.7	52.35	11.88	77
AzoO$(CH_2)_{11}$OH-silica	0.4	41.88	5.87	86
AzoO$(CH_2)_{11}$OH-silica	1.5	59.50	17.69	70
AzoO$(CH_2)_{11}$OH-silica	1.7	52.07	14.26	73

2.2 Determination of Azo-grafting density

Table S3: Elemental analysis results confirming the modulation of grafting density via the concentration of azobenzene derivative used in the thermal grafting process. Results are given for AzoOH-silica, AzoO$(CH_2)_3$OH-silica and AzoO$(CH_2)_{11}$OH-silica modified using three different concentrations corresponding to 1, 3 and 5 molecules/nm^2 of the total surface area. The grafting density was calculated from the % nitrogen in the structure and using surface area for the fumed silica given by the manufacturer (200 m^2/g). * % carbon was used instead as nitrogen showed 0%

	Molecules/nm^2 (synthesis)	%C ± 0.3%	%H ± 0.3%	%N ± 0.3%	Molecules /nm^2
AzoOH	1	2.45	0.18	0.00	0.5*
	3	6.43	0.28	0.96	1.0
	5	9.79	0.67	1.50	1.5
AzoO$(CH_2)_3$OH	1	4.45	0.39	0.63	0.6
	3	11.40	1.33	1.42	1.4
	5	11.23	1.59	1.71	1.7
AzoO$(CH_2)_{11}$OH	1	4.27	0.44	0.37	0.4
	3	13.93	1.28	1.36	1.5
	5	14.58	1.51	1.61	1.7

2.3 Particle Size by Dynamic Light Scattering

Table S4. Dynamic light scattering (DLS) data confirming that the Z-average hydrodynamic diameter (D_h) of fumed silica particles remains largely unchanged (200 nm ± 60 nm) after the grafting reaction. Azo-silica samples were dispersed in either water or *2-propanol depending on their ability to disperse.

	Grafting Density (Molecules/nm^2)	**D_h (nm)**	**Polydispersity Index**
AzoOH	0.5	147.8 (± 0.1)	0.11
	1.0	198.4 (± 1.9)	0.18
	1.5	205.1 (± 4.8)	0.28
$AzoO(CH_2)_3OH$	0.6	186.1 (± 1.8)	0.26
	1.4*	200.4 (± 2.8)	0.18
	1.7*	200.1 (± 0.7)	0.17
$AzoO(CH_2)_{11}OH$	0.4	205.1 (± 4.2)	0.22
	1.5*	221.9 (± 0.6)	0.21
	1.7*	219.3 (± 1.5)	0.27

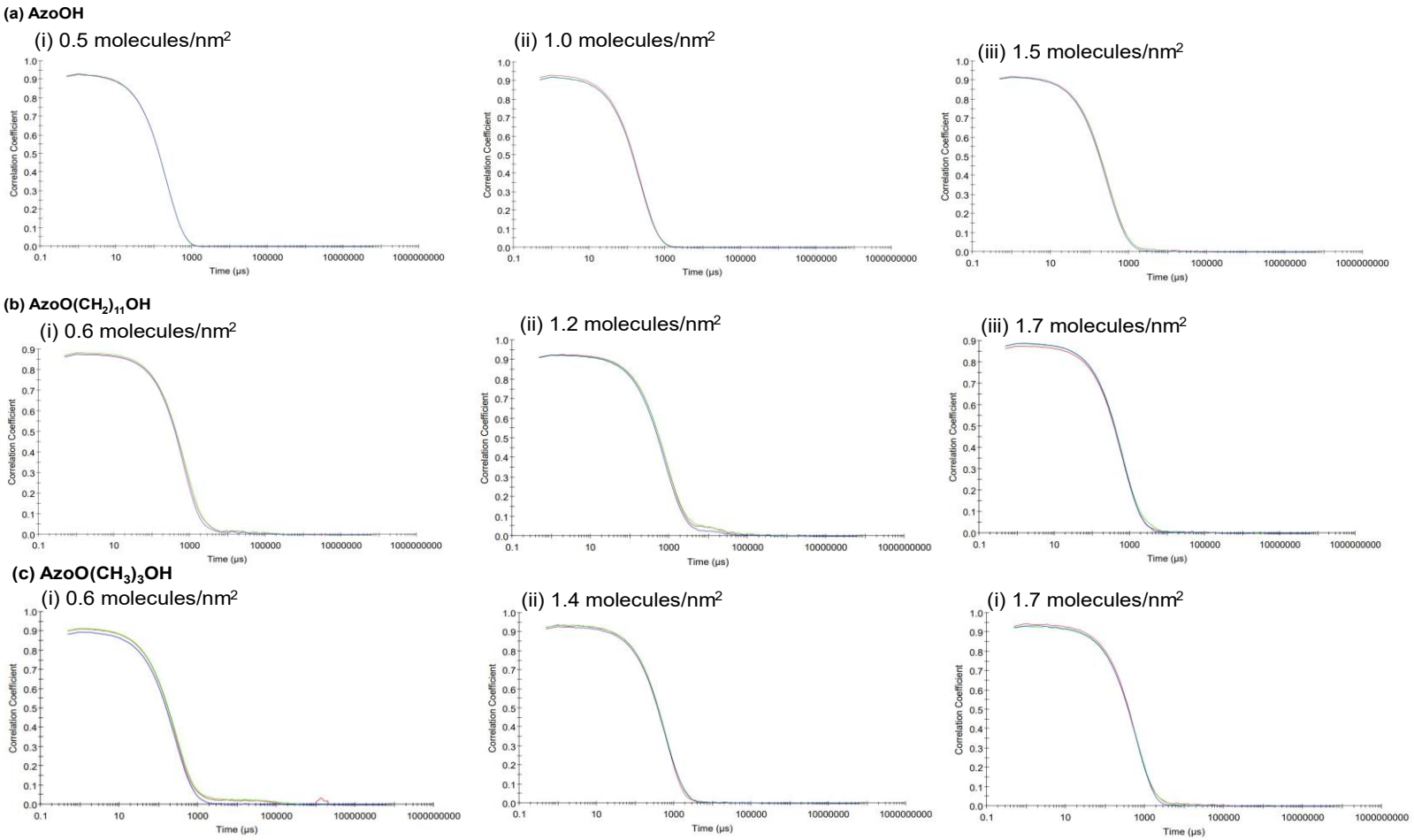

Figure S8. DLS correlograms for Azo-silica samples dispersed in either water or 2-propanol confirming that the samples are largely monodisperse post-grafting. Spectra are of (a) AzoOH-silica, (b) AzoO(CH2)3OH-silica and (c) AzoO(CH2)11OH-silica modified at three different grafting densities (i, ii, and iii)

3 Processing of Microscopy Data.

Microscopy images were analysed using a custom application that uses the circle Hough-transform to detect the presence of circular structures in the images.[2] Due to the density of circles present in the image, a tiling algorithm was used to speed up processing. A list of x, y coordinates and radii were returned which was further processed by removing outliers (z score < 3) and the radii in pixels converted to diameter in microns.

Table S5. Average droplet diameters of particle-stabilised water in oil (W/O) diethyl adipate emulsions obtained by optical microscopy. The polydispersity (PDI) is given as the square of the standard deviation divided by the the average droplet diameter. *Indicates non-spherical emulsions were formed (highly variable droplet size). -Indicates that emulsions did not remain stable after *ca.* 24 h.

			Particle conc. /mg ml^{-1}			
Sample	**Azo grafting density (molecules/nm^2 (EA))**	**UV irradiated?**	**0.0025**	**0.005**	**0.01**	**0.05**
			Average Droplet Diameter / μm (PDI)			
AzoOH-silica	0.5	N	*	*	*	*
		Y	*	*	*	*
	1.0	N	226.33 (0.10)	99.29 (0.06)	56.41 (0.15)	26.92 (0.20)
		Y	161.83 (0.10)	72.41 (0.23)	50.23 (0.13)	24.88 (0.07)
	1.5	N	176.67 (0.05)	117.00 (0.19)	66.90 (0.09)	43.22 (0.19)
		Y	244.76 (0.23)	95.37 (0.09)	71.11 (0.08)	30.56 (0.12)
Azo(CH_2)$_3$OH-silica	0.6	N	189.36 (0.17)	114.29 (0.16)	51.73 (0.23)	37.20 (0.12)
		Y	214.01 (0.22)	93.88 (0.12)	59.30 (0.09)	36.46 (0.08)
	1.4	N	-	218.72 (0.10)	115.55 (0.15)	76.53 (0.07)
		Y	-	329.86 (0.09)	81.52 (0.13)	71.71 (0.07)
	1.7	N	-	157.24 (0.12)	74.81 (0.11)	61.45 (0.26)
		Y	-	87.89 (0.07)	71.42 (0.08)	167.32 (0.19)
Azo(CH_2)$_{11}$OH-silica	0.4	N	392.51 (0.08)	123.41 (0.16)	55.44 (0.11)	35.89 (0.19)
		Y	515.59 (0.47)	243.25 (0.04)	83.32 (0.11)	39.25 (0.18)
	1.5	N	-	-	-	-
		Y	-	249.42 (0.07)	162.66 (0.09)	65.10 (0.40)
	1.7	N	-	-	-	-
		Y	-	410.14 (0.27)	141.51 (0.11)	61.43 (0.22)

4 Stability Study

The stability of the emulsions was assessed by tracking changes in the volume fraction of the aqueous phase, and the resolved oil and water phases as a function of time *i.e.,* the volume that rises to the surface or settles to the bottom by coalescence and sedimentation. The droplet radii were also measured by optical microscopy and are plotted in Figure S13. Emulsions were prepared in either diethyl adipate or n-hexadecane at a particle concentration of 10 mg ml^{-1}. *n*-hexadecane is a non-polar oil which does not show solubility in water and therefore does not show the same self-stabilising effect as diethyl adipate with silica particles.[3,4]

For the adipate emulsions, oil/water is resolved in the first 7 days before reaching a plateau where the emulsion remains stable (Figure S9). The fraction of oil resolved is typically greater than the water, suggesting that sedimentation, as opposed to coalescence, is the main mechanism for destabilisation.[5] Typically, the more hydrophobic emulsions (higher grafting density) show increased sedimentation and coalescence. More hydrophobic particles also form emulsions with larger droplet radii and greater polydispersity (ESI, Figure S9). This is due to greater aggregation of the particles in the oil phase. Despite the changes in the volume of oil and water phases resolved with time, no significant change in the droplet size and dispersity was observed.

The analogous hexadecane systems follow broadly similar trends (Figure S10), where emulsions formed with more hydrophobic particles show greater destabilisation in the first 7 days and form larger, more polydisperse droplets. The main difference is that all emulsions remain stable and O/W emulsions are now accessed by the most hydrophilic particles (see Table S6). This increased stability compared to diethyl adipate emulsions and ability to form O/W emulsions agrees with the dispersion tests (Table 1, main paper). Both W/O and W/O were also found to resolve different phases with time, *i.e.,* $AzoO(CH_2)_3OH$ (0.5 molecules /nm^2) forms O/W emulsions and resolves primarily water whereas $AzoO(CH_2)_{11}OH$ (1.5 molecules/nm^2) is more hydrophobic, forms W/O emulsions and resolves primarily oil over time, suggesting creaming and sedimentation, respectively. None of the emulsions were found to show significant changes upon UV irradiation suggesting that in hexadecane the hydrophobicity of the particles is not near enough to any of the boundary points identified in Figure 1 (main paper).

Table S6. Type of emulsion formed when making emulsion with either diethyl adipate or hexadecane oil. All stable diethyl adipate emulsions are W/O type. For n-hexadecane emulsions, a change from oil in water (O/W)to W/O type is seen for the most hydrophobic particles.

		Diethyl Adipate Emulsion Type		***n*-Hexadecane Emulsion Type**	
	Grafting Density (Molecules/nm^2)	***No UV***	**UV**	**No UV**	**UV**
AzoOH	0.5	W/O	W/O	O/W	O/W
	1.0	W/O	W/O	O/W	O/W
	1.5	W/O	W/O	O/W	O/W
$AzoO(CH_2)_3OH$	0.6	W/O	W/O	O/W	O/W
	1.4	W/O	W/O	W/O	W/O
	1.7	W/O	W/O	W/O	W/O
$AzoO(CH_2)_{11}OH$	0.4	-	W/O	O/W	O/W
	1.5	-	W/O	W/O	W/O
	1.7	W/O	W/O	W/O	W/O

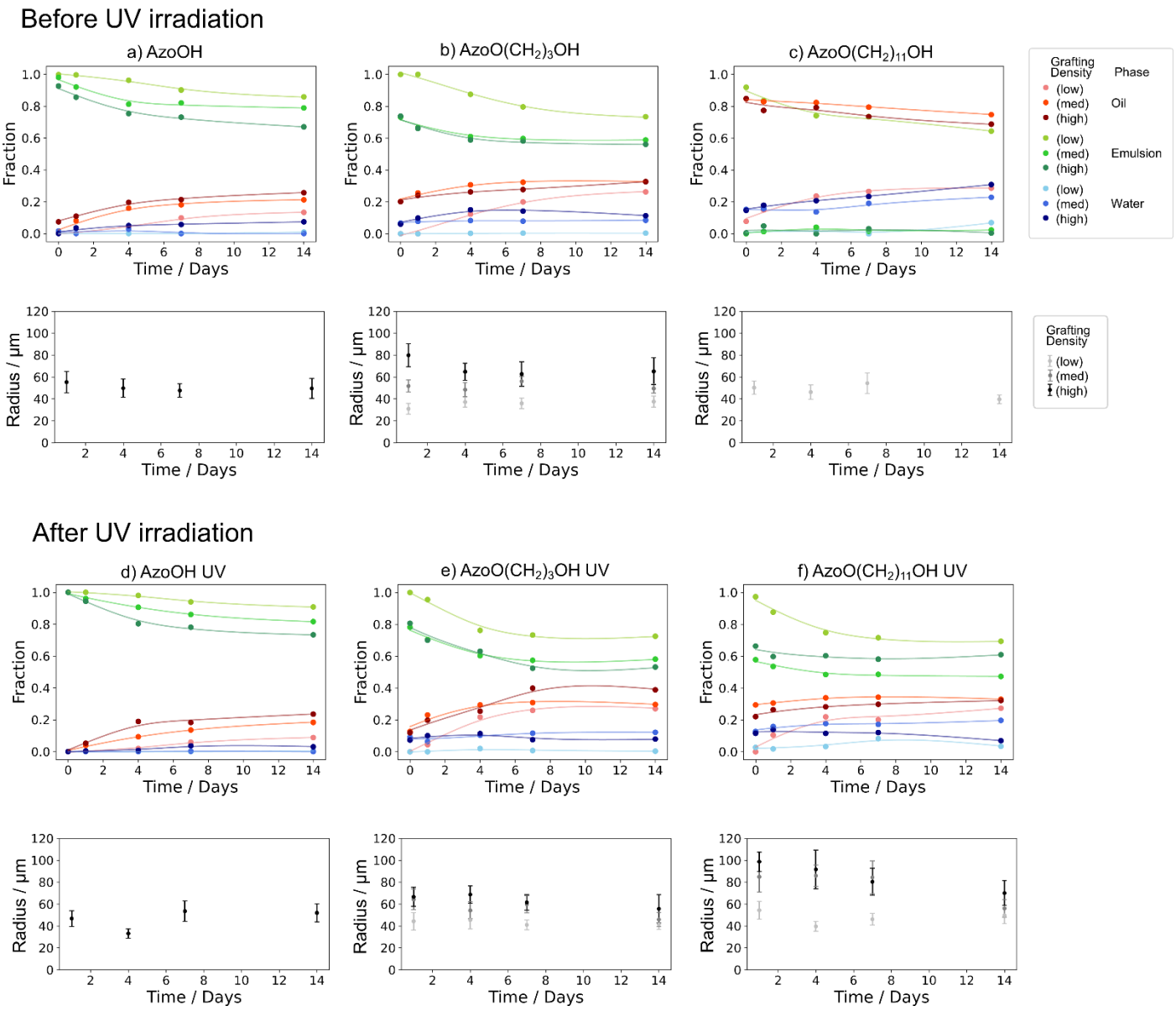

Figure S9. Stability of diethyl adipate emulsions, before and after UV irradiation, stabilised with (a, d) AzoOH, (b,e) AzoO$(CH_2)_3$OH or (c,f) Azo$(CH_2)_{11}$OH particles (10 mg mL^{-1}). The top row of figures in each panel show changes the volume fraction of azo-silica emulsion (green), water (blue) and diethyl adipate (red) resolved between 0 to 14 days after emulsions were made. Darker shades represent higher grafting densities (given in molecules/nm^2) (AzoOH*:* low (0.5), medium (1.0), high (1.5); AzoO$(CH_2)_3$OH: low (0.6), medium (1.4), high (1.7); AzoO$(CH_2)_{11}$OH: low (0.4), medium (1.5), high (1.7)). A correlation between increasing hydrophobicity and decreasing stability of the emulsion phase is observed. The bottom row of figures in each panel shows the corresponding change in droplet radii with time; the error bars reflect the variation in size distribution by image analysis. Low and medium grafted-AzoOH-silica samples (0.5 and 1.0 molecules/nm^2) are excluded as they formed non-spherical droplets. Azo$(CH_2)_{11}$OH (0.4 and 1.5 molecules/nm^2) did not form a stable emulsion without UV irradiation. Overall, more hydrophilic (more stable) particles form smaller, less polydisperse emulsions.

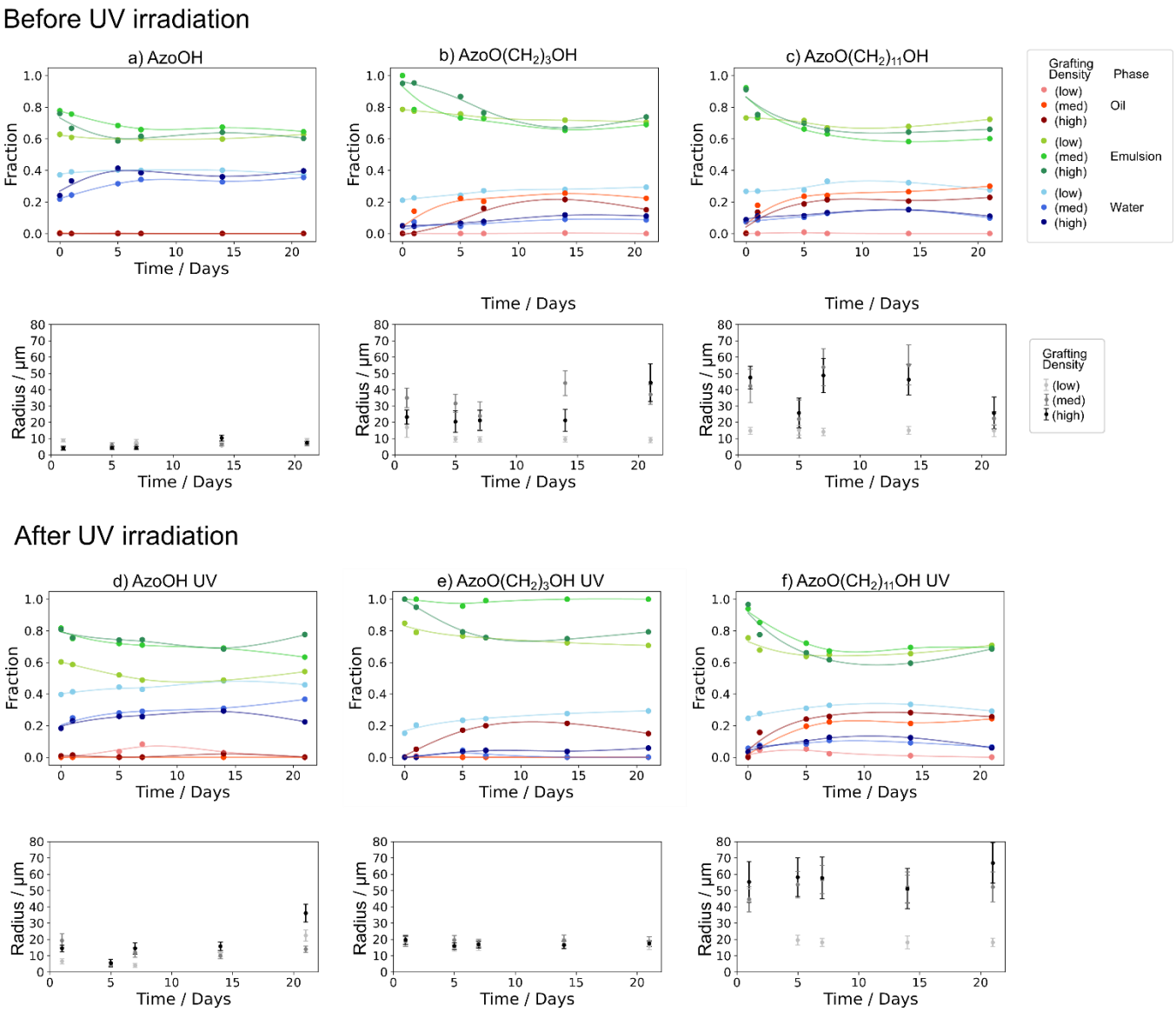

Figure S10. Stability of n-hexadecane emulsions, before and after UV irradiation, stabilised with (a, d) AzoOH, (b,e) AzoO$(CH_2)_3$OH or (c,f) Azo$(CH_2)_{11}$OH particles (10 mg mL^{-1}). The top row of figures in each panel show changes the volume fraction of azo-silica emulsion (green), water (blue) and *n*-hexadecane (red) resolved between 0 to 21 days after emulsions were made. Darker shades represent higher grafting densities (given in molecules/nm^2) (AzoOH*:* low (0.5), medium (1.0), high (1.5); AzoO$(CH_2)_3$OH: low (0.6), medium (1.4), high (1.7); AzoO$(CH_2)_{11}$OH: low (0.4), medium (1.5), high (1.7)). A correlation between increasing hydrophobicity and increasing stability of the emulsion phase is seen for O/W emulsions and the converse is seen for W/O emulsions. The bottom row of figures in each panel shows the corresponding change in droplet radii with time; the error bars reflect the variation in size distribution by image analysis. Overall, for all particle stabilisers, smaller emulsion droplets are formed compared to the diethyl adipate equivalents, with a lower polydispersity.

5 Oil:Water Fraction Study

The oil:water fraction of the light-responsive diethyl adipate emulsion stabilised with AzoO(CH_2)$_{11}$OH-silica (1.4 molecules/nm^2) was modulated in order to see if the O/W state could be accessed by catastrophic inversion (*i.e.,* native W/O to O/W). Emulsions were prepared at 0.2, 0.4, 0.6 and 0.8 water volume fractions, ϕ_w, using azo-silica particles in both irradiated and non-irradiated states. Of all the particles only UV-irradiated Azo(CH_2)$_{11}$OH-Silica (1.4 molecules/nm^2) at water fractions of 0.2 and 0.4, ϕ_w, produced stable emulsions (Figure S15). Overall, smaller, less polydisperse emulsion droplets are formed at lower water fractions and resolve a greater portion of the oil phase before reaching a stable state.

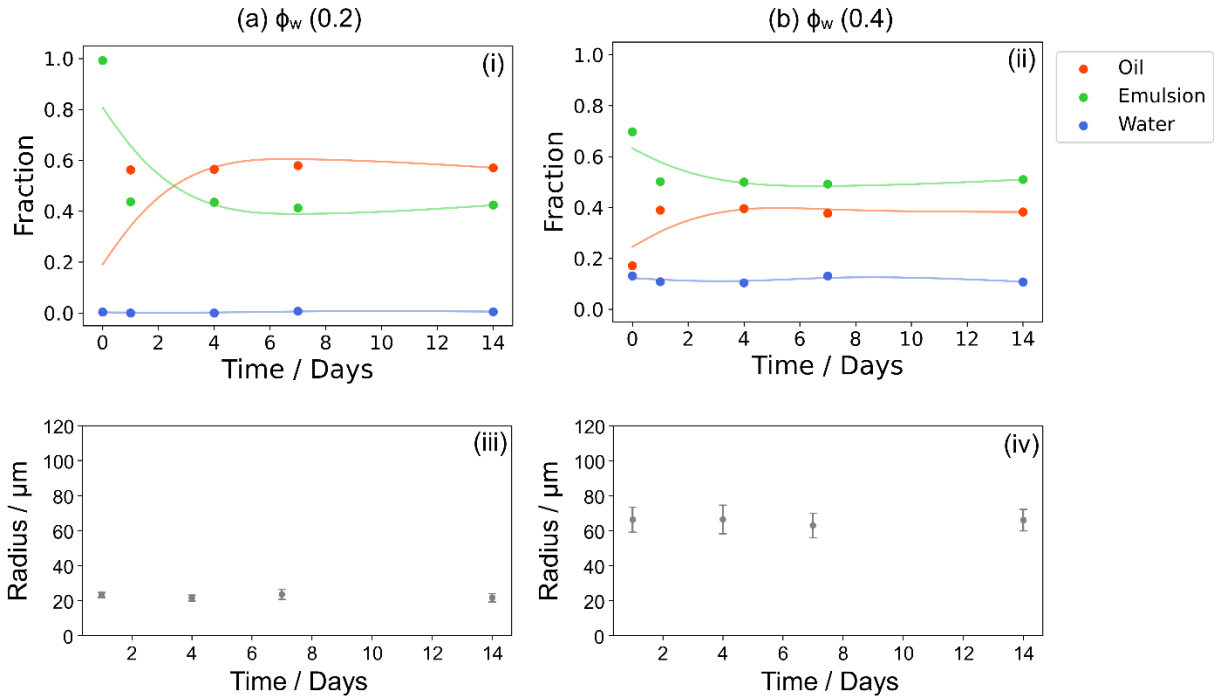

Figure S11. Stability of diethyl adipate emulsions stabilised with AzoO(CH_2)$_{11}$OH-silica (1.5 molecule/nm^2, 10 mg ml^{-1}) particles as a function of water fraction, (a) ϕ_w = 0.2 and (b) ϕ_w = 0.4. All samples were irradiated with UV light pre-emulsification. (i) and (ii) show the volume fraction of azo-silica emulsion (green), water (blue) and diethyl adipate (red) resolved between 0 to 14 days after the emulsions were made. (iii) and (iv) show the corresponding droplet radii over time; the error bars reflect the variation in size distribution by image analysis.

6 Cyclability Study

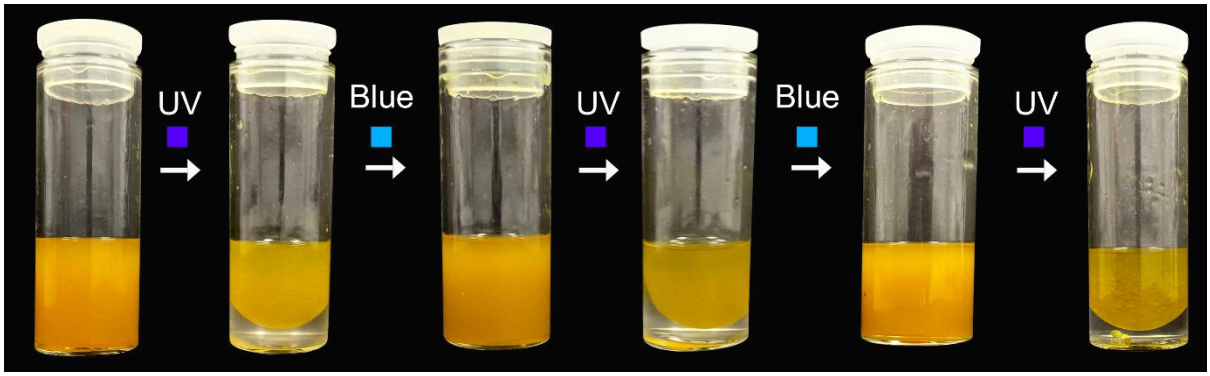

Figure S12. Photographs of a particle-stabilised W/O emulsion (1:1 water : diethyl adipate) prepared using AzoO$(CH_2)_{11}$OH-silica (1.4 molecules/nm^2) at a particle loading of 10 mg mL^{-1} relative to H_2O. The images show cyclability between stable (one distinct phase) and unstable states (two distinct phases). The sample was irradiated with either blue light with stirring or UV light with stirring, followed by homogenisation.

7 Surface Energy Estimation

Contact angle data were acquired for each Azo-silica sample using 4 different test liquids - water, glycerol, ethylene glycol and α-bromonaphthalene. Powder samples were adhered to a glass slide and a minimum of 3 repeats taken with each liquid, acquiring the angle θ_{sl} over 15 seconds. Equilibrium measurements could not be obtained due to sinking of test liquids into the sample. To account for this, an initial contact angle at time, t = 0 was obtained by first finding the linear region of each t vs θ plot, by minimising the chi-squared value of a linear fit, and then taking the intercept. Liquid-air surface energies γ_l along with polar γ_l^p and dispersive γ_l^d contributions are given in Table S5.

Table S7. Literature surface energy values γ_{la} for test liquids used in in the estimation of the surface energy of the Azo-silica particles and calculation of the oil-water contact angle, along with polar γ_l^p and dispersive components γ_l^d.

Liquid	γ_l **/mJ m^{-2}**	γ_l^d **/ mJ m^{-2}**	γ_l^p **/ mJ m^{-2}**
Water[6]	72.8	26.4	46.4
Glycerol[6]	63.4	37.0	26.4
Ethylene glycol[6]	47.7	22.4	34.6
α-Bromonaphthalene[5]	44.4	44.4	0.0
Diethyl adipate[3]	31.7	19.3	12.4
Silicone oil (100 mPa.S)[7]	21.4	20.5	0.9
Hexadecane[5]	27.8	27.8	0.0

The surface energy (γ_s) was obtained by comparing observed contact angles (θ_{sl} – expressed here as θ_{exp} for a given liquid i). with those calculated using Equation 4 (main text) θ_{calc} and iterating over a γ_{sp}- γ_{sd} parameter space (resolution 250 x 250, γ_s^d0 - 50 mJ m^{-2} , γ_s^p 0 - 25 mJ m^{-2}). A three-dimensional goodness of fit plot was then produced using Equation S2, accounting for the variance v_i in the contact angle measurements.

$$goodness\ of\ fit = 1 - \sum \frac{1}{v_i}\left(\theta_{exp^i} - \theta_{calc^i}\right)^2 \quad \text{(S2)}$$

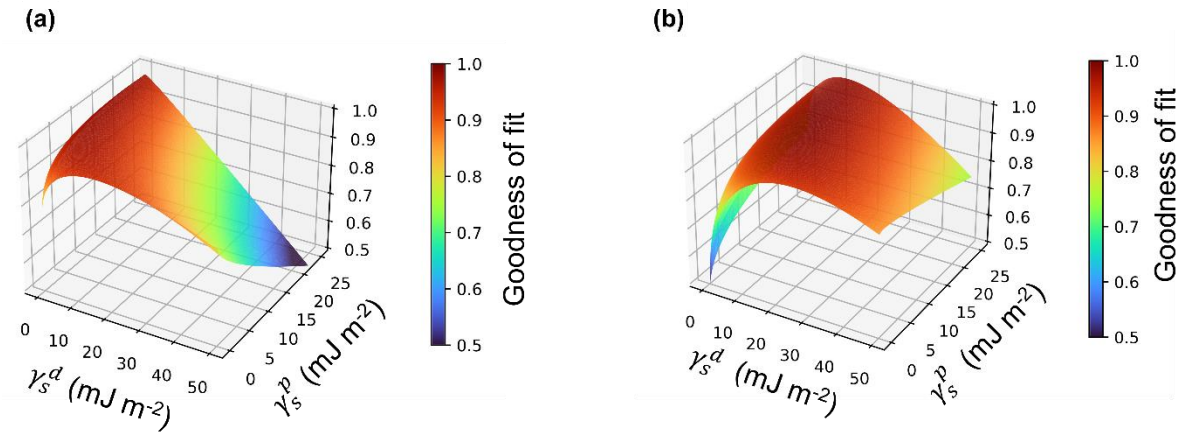

Figure S13. Representative surface energy 'goodness of fit' plots for (a) AzoO$(CH_2)_3$OH-silica-(1.7 molecules/nm^2) and (b) AzoOH-silica (1.5 molecules/nm^2) samples following irradiation UV light, showing low (6.9 ± 1.3 mJ m^{-2}) and high (28.3 ± 6.2 mJ m^{-2}) estimated surface energies, respectively.

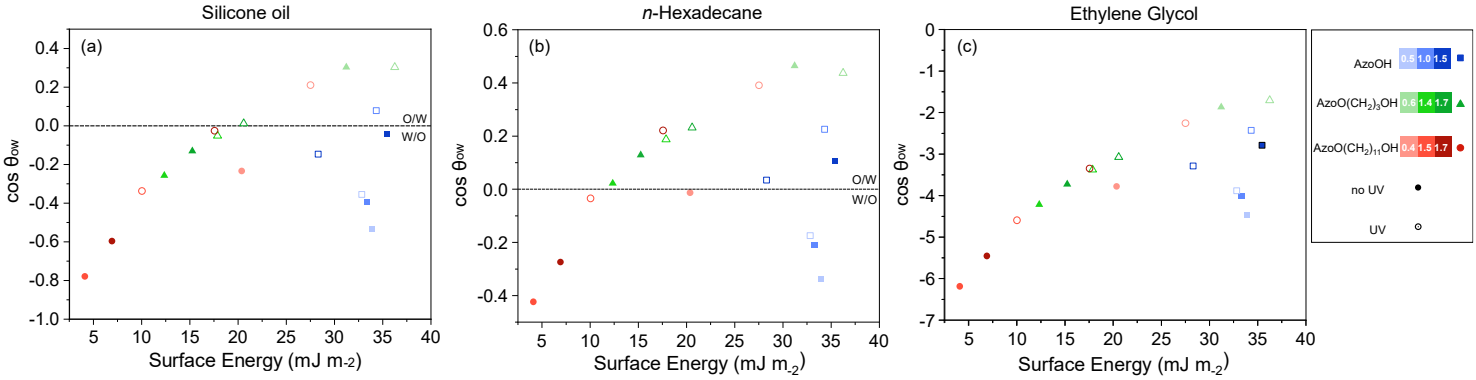

Figure S14. Comparison between surface energy γ_s and predicted cosθ_{ow} for (a) silicone oil and (b) hexadecane and (c) ethylene glycol showing a shift in cos θ_{ow} to lower and higher negative values, respectively (compared to diethyl adipate - Fig. 4 main text) indicating more or less stable emulsions are formed with θ_{ow} closer and further from the optimal 90°. Shades of each colour represent the grafting densities for a given Azo derivative. Hollow shapes indicate that samples were irradiated with UV light prior to measurement.

8 Surface coverage calculations

For each of the diethyl adipate W/O emulsions, linear regression was performed on a particle conc. vs 1/D plot (fitting Equation 5 main text), weighting each point by the median average dispersity for a given mass. Typically, masses used were 2.5, 5, 7.5, 10 and 20 mg and at least 3 stable emulsions were required to perform fitting. Surface coverage was then calculated as described in the main text. Two example plots are given below, at the two distinct surface coverages seen in this investigation/

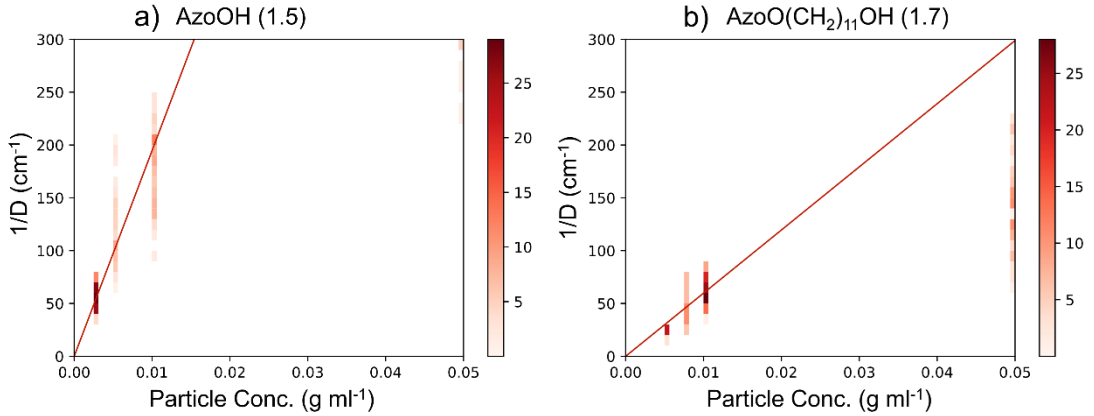

Figure S15. Sample plots for (a) AzoOH-silica-(1.5 molecules/nm^2) and (b) AzoO$(CH_2)_{11}$OH-silica-(1.5 molecules/nm^2) W/O emulsions showing difference in gradient, and therefore surface coverage, for plots of 1/D vs particle concentration (relative to the oil phase) used to make particle-stabilised emulsions. A lower gradient is associated with a greater surface coverage.

9 References

1 S. Peng, Q. Guo, P. G. Hartley and T. C. Hughes, *J. Mater. Chem. C*, 2014, **2**, 8303–8312.

2 Hough-scan, https://github.com/KRichardsF/Hough-Scan, (accessed 28 May 2021).

3 J. Frelichowska, M.-A. Bolzinger and Y. Chevalier, *Colloids Surfaces A Physicochem. Eng. Asp.*, 2009, **343**, 70–74.

4 B. P. Binks and D. Yin, *Soft Matter*, 2016, **12**, 6858–6867.

5 B. P. Binks and S. O. Olusanya, *Chem. Sci.*, 2017, **8**, 708–723.

6 C. Rulison, *KRÜSS Technical Note 306e*, Hamburg, 1999.

7 B. P. Binks and A. T. Tyowua, *Soft Matter*, 2016, **12**, 876–887.